

**STRESS STATE MODELLING FOR COMPOSITE
TRACTIVE ELEMENT WITH BREAKAGES OF CABLE
REINFORCEMENT AND CHANGE IN MECHANICAL
PROPERTIES OF ELASTOMER SHELL**



Ivan BELMAS

Dr. Sc. (Tech.), Prof., Head of Department of Mechanical Engineering Technology, Dniprovsk State Technical University, Kamianske, Ukraine



Dmytro KOLOSOV

Dr. Sc. (Tech.), Prof., Head of Department of Mechanical and Biomedical Engineering, Dnipro University of Technology, Dnipro, Ukraine



Serhii ONYSHCHENKO

Cand. Sc. (Tech.), Associate Professor of Department of Mechanical and Biomedical Engineering, Dnipro University of Technology, Dnipro, Ukraine



Olena BILOUS

Cand. Sc. (Tech.), Associate Prof., Associate Prof. of Department of Industrial Engineering, Dniprovsk State Technical University, Kamianske, , Ukraine



Hanna TANTSURA

Cand. Sc. (Tech.), Associate Prof., Associate Prof. of Department of Industrial Engineering, Dniprovsk State Technical University, Kamianske, Ukraine

Abstract. The purpose of research is determination of a dependency of a stress state for composite elastomer-cable tractive element with a broken structure on a nonlinear dependency of shear modulus on deformations in the elastomeric shell. Research methodology is in analytical solution of a model of a composite tractive element with disturbed structure and a deformation-dependent shear modulus of an elastomeric shell. Results are in constructing an algorithm for determining a stress state of a composite tractive element with broken structure and a deformation-dependent shear modulus. Scientific novelty is in determining a character of dependency for a stress state of a composite tractive element on a nonlinear dependency of shear modulus on deformations. Practical application of research is in a possibility to determine the dependency of a stress state of a composite elastomer-cable tractive element on a nonlinear shear modulus allows considering the effect of this phenomenon on the tractive element strength and ensures an increase of its operational safety.

Introduction

Continuous improvement of technical systems in the fields of mining technologies [1-9], transportation and hoisting [10-12], deep-sea mining [13, 14], and dynamics of technical systems [15-19] facilitate wider and more thorough development of analytical and computational simulation methods of processes and phenomena occurring within the systems. Currently, researchers in many countries are conducting complex scientific studies aimed at developing methods and means of modernizing lifting and transporting complexes with the aim of increasing operational efficiency and safety of mining transport equipment. Composite elastomer-cable tractive elements, in particular rubber-cable ropes (RCR), also known as steel cord belts, are widely used in hoisting and transporting machines [20-24]. At the same time, these tractive elements have significant lengths. Conveyor belts of a closed shape are created by connecting ends of belts. Cables at belt ends in such connections are not mechanically connected and interact through rubber layers. Damage accumulates in ropes during use. One type of damage is rupture of one of reinforcing elements (cables). Rupture of continuity of cables and presence of non-continuing cables, in accordance with the Saint-Venant's principle, are sources of disturbance of a stress-strain state in a rope (belt).

State of Question and Research Problem

Rope strength in the cross-section of cable breakage is much lower [25-27], it is also lower in butt joints [28]. In paper [29], it is suggested to determine a stress-strain state of spatial structures reinforced with parallel elements by means of electrical modelling. A

method of determining characteristics of materials with a system of regularly arranged parallel reinforcing elements is suggested in the article [30]. The papers [31-40] are devoted to investigation of features of a rope (belt) stress state, considering its interaction with structural elements of a machine. Experience indicates that there is a nonlinear dependency of stresses in elastic materials on their deformations, and rubber is no exception to this. Rubber layers in rubber-cable ropes ensure the connection of cables, determine a mechanism of redistribution of forces between the cables, which affects the operational characteristics of the entire rope. In these papers, the issue of a nonlinear law of rubber deformation is not considered. At the same time, it constitutes an actual scientific and technical problem of considering the specified feature during the design and continuous control of the condition of hoisting and transporting machines with a rubber-cable tractive element. The solution allows considering the influence of deformation character in rubber on rope strength and provides a possibility of increasing operational safety of rubber-cable ropes (belts).

Generally, the dependency graph of stresses on deformations has a shape of a curved line. The main factor in the occurrence of shear stresses in rubber layers of a rope or belt is breakage of continuity of cables. Discontinuity of cables occurs in the event of cable breakage and in butt joints of rubber-cable ropes and belts. In butt-joint connections, no cables at both ends of the connected belts continue. A cable break or a cable end is a source of stress-strain state disturbance in a rope (belt). Well-known studies [26] indicate that deformations of rubber take place practically only in the layers adjacent to the broken cable. Deformation values are maximum in the cross-section of cable continuity breakage and decrease exponentially with increasing distance from the specified cross-section.

Consideration of Natural Changes in Mechanical Properties of Elastic Shell on Stress-Strain State of a Rope

Loading forces on cables and their displacements without considering rubber aging, according to [26] are determined by dependencies

$$p_i = E F \sum_{m=1}^{M-1} \left(A_m e^{\beta_m x} - B_m e^{-\beta_m x} \right) \beta_m \cos(\mu_m (i - 0.5)) + P, \quad (1)$$

$$u_i = \sum_{m=1}^{M-1} \left(A_m e^{\beta_m x} + B_m e^{-\beta_m x} \right) \cos(\mu_m (i-0.5)) + \alpha + \frac{P x}{E F}, \quad (2)$$

where M is amount of cables in a rope, i is cable number ($1 \leq i \leq M$); A_m, B_m are integration constants; E, F are, respectively, reduced tensile modulus of elasticity and cross-sectional area of a cable in a rope (belt); x is coordinate axis directed along the rope, P is average load

on a cable in a rope; $\beta_m = \sqrt{2 \frac{G b k_G}{(h-d) E F} [1 - \cos(\mu_m)]}$; $\mu_m = \frac{\pi m}{M}$;

h is distance between cables; b is rope thickness; d is cable diameter; G is shear modulus of elastic (rubber) layer connecting the cables, k_G is coefficient of shape influence of rubber located between cables on shear rigidity; α is cable displacement as a rigid body.

Natural change in mechanical properties during aging process of an elastic shell is associated with a change in modulus of elasticity and shear modulus. According to (1) and (2), shear modulus affects a stress-strain state of a rope. Assume that a law of change of shear modulus of an elastic (rubber) layer is known. Its value is given by the following expression

$$G = G_0 f(t), \quad (3)$$

where G_0 is shear modulus right after rope (belt) production ($t=0$).

Formulate a physical model of rope deformation made of M cables of considerable length. Cable with number J has a continuity breakage. This breakage is located at an infinitely large distance from rope edges. Rope is loaded with a tensile force. Tensile force ensures an average loading on cables equal to one. Direct an x -axis along the rope. Place axis origin point at a cross-section of cable breakage. Consider a rope part for which ($0 \leq x \leq \infty$).

From a condition of limited displacements of cables and limited loading forces on cables for an infinite growth of x -coordinate, assume that $A_m=0$. Consider rope displacement as a rigid body equal to zero. Then, expressions (1) and (2) obtain the following forms

$$p_i = -E F \sum_{m=1}^{M-1} B_m e^{-\beta_m^* x} \beta_m^* \cos(\mu_m (i-0.5)) + P, \quad (4)$$

$$u_i = \sum_{m=1}^{M-1} B_m e^{-\beta_m^* x} \cos(\mu_m (i-0.5)) + \frac{P x}{EF}, \quad (1 \leq i \leq M), \quad (5)$$

where $\beta_m^* = \sqrt{\frac{2G_0 f(t) b k_G}{(h-d)EF} [1 - \cos(\mu_m)]}$.

Displacements of all cables, except for the broken one, in the cross-section $x=0$ are absent. Displacement of a broken cable is denoted as U_0 . Displacements of cables in the cross-section $x=0$ are defined as product of U_0 and δ -function on a limited axis length of discrete cable numbers. This makes it possible to determine the vector of unknown constants of integration from expression (5) through one unknown quantity

$$B_m = \frac{2}{M} U_0 \cos(\mu_m (J-0.5)). \quad (6)$$

The unknown U_0 is determined from a condition that a loading force (4) of a broken cable is zero

$$U_0 = \frac{P M}{2 EF \sum_{m=1}^{M-1} \cos^2(\mu_m (J-0.5)) \beta_m^*}. \quad (7)$$

Expressions (4) - (7) make it possible to determine a stress-strain state of a rope of considerable length on a hoisting machine and a conveyor belt of considerable length in case of breakage of an arbitrary cable, considering the aging period of their elastic shell at the moment of cable breaking.

Known displacements of cables (5) allow determining relative shear of cables. Difference in shear of adjacent cables is accompanied by occurrence of tangent stresses in an elastic shell. The tangent stresses are at their maximum values in a plane of axes of rope cables. The distances between the nearest points on surfaces of adjacent cables are minimal in this plane. Tangents of shear angles are determined by the following expression

$$\tan(\gamma_j) = \frac{u_j - u_{j+1}}{h}, \quad (1 \leq j < M), \quad (8)$$

where j is layer number.

For a rope of RCR-3150 type consisting of five cables, determine a distribution of internal forces and tangents of shear angles for an elastic shell in a plane where centers of cross-sections in cables are located. Assume that as a result of natural changes in rubber properties, a shear modulus has doubled. Apply an external load so that the average load on cables is equal to one. The noted internal loading forces on cables in this case are equal to a coefficient of uneven loading on cables. Results for cases $f(T)=2$ (curve 1) and $f(0)=1$ (curve 2) are indicated in Fig. 1 and 2.

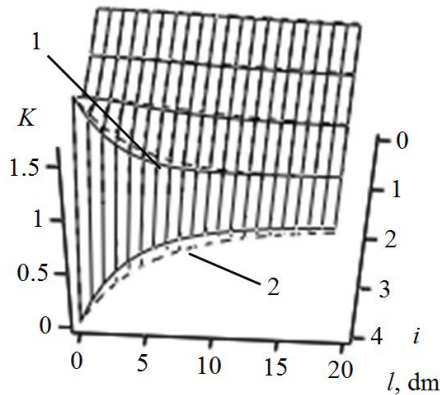


Fig. 1. Distribution of coefficients of uneven loading on cables with numbers i along rope length l

According to graphs shown in the Figure 1, loads on cables caused by continuity breakage in of one of them lead to a local redistribution of forces practically only between two cables - the broken one and the one adjacent to it. Accordingly, in a case of breakage in a non-extreme cable, the forces practically change only in three cables - the broken one and two adjacent ones to it. The forces change significantly over a length of up to 2 m. The extreme values of internal loading forces on cables do not depend on change in shear modulus of rubber material over time.

Distribution of tangents of shear angles in rubber (Fig. 2) also indicates an insignificant effect on rubber shear angles between cables.

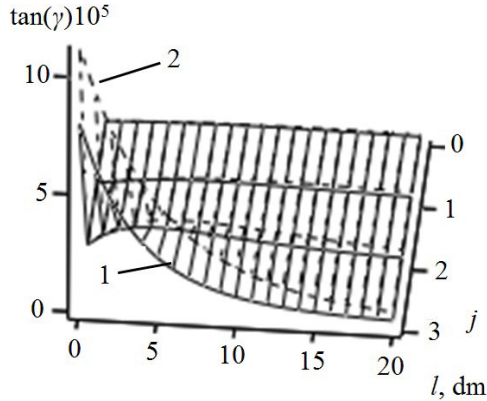


Fig. 2. Distribution of maximum tangents of shear angles in material located in layers with numbers j between cables along rope length l

Significant rubber shear is observed only between the broken cable and the one adjacent to it along the cable length. Shear angles of rubber between other cables are much smaller compared to shears in a zone of local redistribution of forces and stresses. They change little because of rubber aging over time. Length of conveyors and hoisting heights for using rubber-cable ropes and belts exceed 100 m. This makes it possible to consider the above assumption of an infinite rope length and an infinite distance from a cable breakage to a belt (rope) end.

The second feature of influence of operating time on a rope stress-strain state is a local decrease in a value of shear modulus of elastic material in zones of increased stress. Ropes and belts operate under cyclic loads. Each cyclic load is accompanied by accumulation of residual strain. Rubber shell between cables, due to its much lower tensile strength than that of cables, practically is not loaded until the moment of cable breakage. There are no residual shear deformations in it.

Consideration of Cable Breakage on Stress-Strain State of Composite Flat Rubber-Cable Rope

A change in a stress-strain state of a belt (rope) as a result of cable breakage leads to occurrence of shear in elastic shell material located between individual cables and accumulation of residual strain. Larger absolute values of total deformations that occur in rub-

ber after a cable breaks lead to larger absolute values of residual strain. According to graphical dependencies shown in Figure 2, local changes in a design of composite flat rubber-cable rope (belt) lead to local changes in their stress-strain state. Investigate the local influence of changes in properties of an elastic material that interacts with a broken cable.

Construction of Model of Rubber-Cable Tractive Element with a Broken Structure and Nonlinear Deformation-Dependent Rubber Shear Modulus

Determining a stress-strain state considering the specified character of deformation changes and considering the nonlinear dependency of shear displacements on rubber shear stresses is a complex mathematical problem. Let's simplify it. Assume that the dependency of rubber shear stresses on its deformations is piecewise linear and consists of two parts. As in the studies mentioned above, we assume that the cables deform like rods. Rubber is subjected only to shear stress. The rope is infinitely long. It has M cables and is loaded with a tensile force P . The cable numbered j has a continuity breakage. The cross-section with the breakage is at a considerable distance from the rope edges. Rubber shear modulus of layers adjacent to the damaged cable at lengths l_0 is different from the corresponding rubber shear modulus of the remaining layers. The linear size l_0 is much smaller than the rope length, on which the stress state is changed because of a cable breaking. Direct the coordinate axis along the rope. Its origin ($x = 0$) is located at the point where the cable breaks. Since the cross-section ($x = 0$) is a cross-section of symmetry, the displacements of cables are symmetrical. At the same time, the cross-sections of all cables except the ends of the broken cable do not move. A gap is formed between the ends of the damaged cable. Let's denote the displacement of the end of the damaged cable U_0 .

Let's single out a part of length $l_0(0 \leq l_0)$. Consider it the first one. Consider the part for which ($x > l_0$) the second part. The first part of the rope is divided into three stripes with an unchanged number of cables in each. Include stripes that do not have a broken cable into the structure of the two extreme stripes. Give them numbers one and three. The rope part with the broken cable and the cables adjacent to it will be included in the structure of the second stripe (Fig. 3).

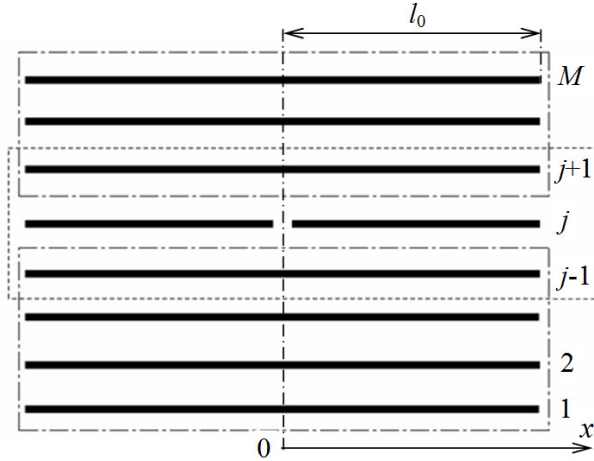


Fig. 3. Rope part with a broken cable

Consider the specified stripes as separate belts. A characteristic feature of such rope stripes is that the properties of elastic material between the rope stripes do not change. Shear modulus of rubber in layers between cables is not variable in our case. This allows using the conditions of their equilibrium and the form of solutions for stripes [26], considering the number of cables in stripes and properties of elastic shell. Let's make expressions that allow determining the internal forces in cables and their displacements. Write down the expressions for the extreme stripes in similar forms. In the expressions, we will use additional indices to assign the parameters to one or another rope stripe. Take into account that cross-sections of cables of the extreme stripes do not move when $(x = 0)$.

Assumed Forms of Solution

For a rope stripe with cable numbers $(1 \leq i \leq j-1)$

$$p_{1,i} = E F \sum_{m=1}^{j-2} \left[A_m \left(e^{\beta_{1,m} x} + e^{-\beta_{1,m} x} \right) \times \right. \\ \left. \times \beta_{1,m} \cos(\mu_{1,m} (i - 0.5)) \right] + P, \quad (9)$$

$$u_{1,i} = \sum_{m=1}^{j-2} A_m \left(e^{\beta_{1,m} x} - e^{-\beta_{1,m} x} \right) \cos(\mu_{1,m} (i - 0.5)) + \frac{P x}{E F}, \quad (10)$$

where i is cable number in the first stripe;

$$\beta_{1,m} = \sqrt{\frac{2G_0 b}{(h-d)EF} [1 - \cos(\mu_{1,m})]}.$$

For the second rope stripe with cable numbers ($j-1 \leq i \leq j+1$)

$$p_{2,i} = EF \sum_{m=1}^2 \left[\left(A_{m+j-2} e^{\beta_{2,m} x} - B_{m+j-2} e^{-\beta_{2,m} x} \right) \times \right. \\ \left. \times \beta_{2,m} \cos(\mu_{2,m}(i-j-1.5)) \right] + P, \quad (11)$$

$$u_{2,i} = \sum_{m=1}^2 \left[\left(A_{m+j-2} e^{\beta_{2,m} x} + B_{m+j-2} e^{-\beta_{2,m} x} \right) \times \right. \\ \left. \times \cos(\mu_{2,m}(i-j-1.5)) \right] + \frac{Px}{EF}, \quad (12)$$

where $\mu_{2,m} = \frac{\pi m}{3}$; $\beta_{2,m} = \sqrt{\frac{2G_0 b k}{(h-d)EF} [1 - \cos(\mu_{2,m})]}$; k is coefficient, which considers the difference in shear modulus of rubber for the second stripe.

For a rope stripe with cable numbers ($j+1 \leq i < M$)

$$p_{3,i} = EF \sum_{m=1}^{M-j-1} \left[A_{m+j} \left(e^{\beta_{3,m} x} + e^{-\beta_{3,m} x} \right) \times \right. \\ \left. \times \beta_{3,m} \cos(\mu_{3,m}(i-j-1.5)) \right] + P, \quad (13)$$

$$u_{3,i} = \sum_{m=1}^{M-j-1} \left[A_{m+j} \left(e^{\beta_{3,m} x} - e^{-\beta_{3,m} x} \right) \times \right. \\ \left. \times \cos(\mu_{3,m}(i-j-1.5)) \right] + \frac{Px}{EF}, \quad (14)$$

where $\mu_{3,m} = \frac{\pi m}{M-j}$; $\beta_{3,m} = \sqrt{\frac{2G_0 f(t) b k_G}{(h-d)EF} [1 - \cos(\mu_{3,m})]}$.

These solutions correspond to the conditions of influence absence of external factors on extreme cables in stripes on the interval ($0 \leq x \leq l_0$). The cables adjacent to the broken one are included in two stripes – the extreme one and non-extreme one. In the extreme stripes, there are no disturbances in cables adjacent to the broken one, in accordance with solutions of (9), (10) and (13), (14). They are

loaded with only evenly distributed forces. Cables in the cross-section $x = 0$ are immovably fixed. In a general solution, based on the principle of superposition, we add their displacements as cables, which are part of the middle stripe, to displacements of these cables without considering the force of their external load.

The end of the middle cable in the middle stripe is displaced by an unknown amount U_0 under the action of an external force. Let's write the above in a form of a boundary condition for the cross-section $x=0$

$$u_{2,i} = U_0 \begin{cases} 0, & i \neq j, \\ 1, & i = j. \end{cases} \quad (15)$$

According to (15), the law of cable displacements corresponds to the product of displacement of a middle cable and the Dirac function δ . Let's take the Dirac function in a form of a Fourier series on a given segment of cable numbers. From expression (12), we have the following

$$\begin{aligned} & \sum_{m=1}^2 (A_{m+j-2} + B_{m+j-2}) \cos(\mu_{2,m}(i-0.5)) = \\ & = \frac{2}{3} U_0 \sum_{m=1}^2 \cos\left(\frac{3}{2} \mu_{2,m}\right) \cos(\mu_{2,m}(i-0.5)), \quad (i=1,2,3). \end{aligned} \quad (16)$$

From where

$$B_{m+j-2} = \frac{2}{3} U_0 \cos(1.5 \mu_{2,m}) - A_{m+j-2}, \quad (m=1,2). \quad (17)$$

From the condition that a load on the broken cable in the cross-section of breakage is equal to zero from expression (11) we have

$$U_0 = \frac{3P}{2\beta_{2,m} E F \cos^2(1.5 \mu_{2,m})} + 3 \frac{A_{m+j-2}}{\cos(1.5 \mu_{2,m})}. \quad (18)$$

Accordingly, expression (17) takes the form

$$B_{m+j-2} = \frac{P}{\beta_{2,m} E F \cos(1.5 \mu_{2,m})} + 2A_{m+j-2}. \quad (19)$$

Expressions of forces (11) and displacements (12) considering the general numeration of cables in the cross-section of a rope take the following forms

$$p_{2,i} = EF \sum_{m=1}^2 \left[\left(\begin{aligned} &A_{m+j-2} \left(e^{\beta_{2,m}x} - 2e^{-\beta_{2,m}x} \right) \times \\ &\times \beta_{2,m} - \frac{Pe^{-\beta_{2,m}x}}{\cos(1.5\mu_{2,m})} \\ &\times \cos(\mu_{2,m}(i-j-1.5)) \end{aligned} \right) \times \right] + P, \quad (20)$$

$$u_{2,i} = \sum_{m=1}^2 \left[\left(\begin{aligned} &A_{m+j-2} \left(e^{\beta_{2,m}x} + e^{-\beta_{2,m}x} + 0.5 \right) + \\ &+ \frac{P \left(e^{-\beta_{2,m}x} + 0.5 \right)}{\beta_{2,m}EF \cos(1.5\mu_{2,m})} \\ &\times \cos(\mu_{2,m}(i-j-1.5)) \end{aligned} \right) \times \right] + \frac{Px}{EF}. \quad (21)$$

Using (9), (10), (13), (14), (20), (21), we write down the values of forces and displacements as single functions on the finite axis of cable numbers

$$p_i = \frac{2EF}{M} \sum_{n=1}^{M-1} \rho_n(x) \cos(\mu_n(i-0.5)) + P, \quad (22)$$

where $\mu_n = \frac{\pi n}{M-1}$;

$$\rho_n(x) = \sum_{\chi=1}^{j-1} \sum_{m=1}^{j-2} \left[\begin{aligned} &A_m \left(e^{\beta_{1,m}x} + e^{-\beta_{1,m}x} \right) \beta_{1,m} \times \\ &\times \cos(\mu_{1,m}(\chi-0.5)) \cos(\mu_n(\chi-0.5)) \end{aligned} \right] + \\ + \sum_{\chi=1}^3 \sum_{m=1}^2 \left[\left(\begin{aligned} &A_{m+j-2} \left(e^{\beta_{2,m}x} - 2e^{-\beta_{2,m}x} \right) \times \\ &\times \beta_{2,m} - \frac{Pe^{-\beta_{2,m}x}}{EF \cos(1.5\mu_{2,m})} \\ &\times \cos(\mu_{2,m}(\chi-0.5)) \cos(\mu_n(\chi+j-2.5)) \end{aligned} \right) \times \right] +$$

$$\begin{aligned}
& + \sum_{\chi=1}^{M-j-1} \sum_{m=1}^{M-j-1} \left[A_{m+2} \left(e^{\beta_3, m^x} + e^{-\beta_3, m^x} \right) \beta_{3, m} \times \right. \\
& \quad \left. \times \cos(\mu_{3, m} (\chi - 0.5)) \cos(\mu_n (\chi + j - 0.5)) \right] \\
u_i & = \frac{2}{M} \sum_{n=1}^M v_n(x) \cos(\mu_n (i - 0.5)) + \frac{P x}{E F}, \quad (23)
\end{aligned}$$

where

$$\begin{aligned}
v_n(x) & = \sum_{\chi=1}^{j-1} \sum_{m=1}^{j-2} \left(A_m \left(e^{\beta_1, m^x} - e^{-\beta_1, m^x} \right) \times \right. \\
& \quad \left. \times \cos(\mu_{1, m} (\chi - 0.5)) \cos(\mu_n (\chi - 0.5)) \right) + \\
& + \sum_{\chi=1}^3 \sum_{m=1}^2 \left(\left(A_{m+j-2} \left(e^{\beta_2, m^x} + e^{-\beta_2, m^x} \right) + \right. \right. \\
& \quad \left. \left. + \frac{P e^{-\beta_2, m^x}}{\beta_{2, m} E F \cos(1.5 \mu_{2, m})} \right) \times \right. \\
& \quad \left. \times \cos(\mu_{2, m} (\chi - 0.5)) \cos(\mu_n (\chi + j - 2.5)) \right) + \\
& + \sum_{\chi=1}^{M-j-1} \sum_{m=1}^{M-j-1} \left(A_{m+2} \left(e^{\beta_3, m^x} - e^{-\beta_3, m^x} \right) \times \right. \\
& \quad \left. \times \cos(\mu_{3, m} (\chi - 0.5)) \cos(\mu_n (\chi + j - 0.5)) \right).
\end{aligned}$$

Expressions (22), (23) are obtained for the first part of the rope for $(0 \leq x \leq l_0)$. In cross-section $x=l_0$ the considered part of the rope interacts with its second part. Write expressions of forces $(p_{0,i})$ and displacements $(u_{0,i})$ for the second part in the forms [26]. At the same time, we consider that an infinite increase in the value of x -coordinate cannot lead to an infinite increase in the loading forces of cables and their displacements

$$p_{0,i} = -E F \sum_{n=1}^{M-1} B_{0,n} e^{-\beta_n^* x} \beta_n^* \cos(\mu_n (i - 0.5)) + P, \quad (24)$$

$$u_{0,i} = \sum_{n=1}^{M-1} B_{0,n} e^{-\beta_n^* x} \cos(\mu_n (i - 0.5)) + \frac{Px}{EF}; (1 \leq i \leq M), \quad (25)$$

where $\beta_n = \sqrt{\frac{2G_0b}{(h-d)EF} [1 - \cos(\mu_n)]}$.

At the same time, in cross-section $x=l_0$ the conditions of joint deformation of rope parts must be fulfilled

$$p_{0,i} = p_i, \quad (26)$$

$$u_{0,i} = u_i. \quad (27)$$

From expressions (22), (23) and conditions (26), (27), we have equalities

$$B_{0,n} e^{-\beta_n^* l_0} = -\frac{2}{M \beta_n^*} \rho_n; \quad (x = l_0), \quad (28)$$

$$B_{0,n} e^{-\beta_n^* l_0} = \frac{2}{M} \nu_n; \quad (x = l_0). \quad (29)$$

Subtract (29) from (28). We get a system of $N - 1$ equations

$$\sum_{\chi=1}^{j-1} \sum_{m=1}^{j-2} \left(A_m \left(e^{\beta_{1,m} l_0} \left(1 + \frac{\beta_{1,m}}{\beta_n^*} \right) - e^{-\beta_{1,m} l_0} \left(1 - \frac{\beta_{1,m}}{\beta_n^*} \right) \right) \times \right. \\ \left. \times \cos(\mu_{1,m} (\chi - 0.5)) \cos(\mu_n (\chi - 0.5)) \right) + \\ + \sum_{\chi=1}^3 \sum_{m=1}^2 \left(\left(A_{m+j-2} \left(e^{\beta_{2,m} l_0} \left(1 + \frac{\beta_{2,m}}{\beta_n^*} \right) + \right. \right. \right. \\ \left. \left. \left. + e^{-\beta_{2,m} l_0} \left(1 - 2 \frac{\beta_{2,m}}{\beta_n^*} \right) \right) \right) \times \right. \\ \left. \left. + \frac{Pe^{-\beta_{2,m} l_0}}{EF \cos(1.5\mu_{2,m})} \left(\frac{1}{\beta_{2,m}} - \frac{1}{\beta_n^*} \right) \right) \right) \\ \left. \times \cos(\mu_{2,m} (\chi - 0.5)) \cos(\mu_n (\chi + j - 2.5)) \right) +$$

(30)

$$+ \sum_{\chi=1}^{M-j-1} \sum_{m=1}^{M-j-1} \left[A_{m+2} \begin{pmatrix} e^{\beta_{3,m} l_0} \left(1 + \frac{\beta_{3,m}}{\beta_n^*} \right) - \\ -e^{-\beta_{3,m} l_0} \left(1 - \frac{\beta_{3,m}}{\beta_n^*} \right) \end{pmatrix} \times \right. \\ \left. \times \cos(\mu_{3,m}(\chi - 0.5)) \cos(\mu_n(\chi + j - 0.5)) \right].$$

The solution of obtained system of equations (30) allows determining the unknown constants and internal loading forces of cables, and their displacements. The known displacements make it possible to determine tangential stresses in material of the elastic shell located between the cables, which are directly proportional to the tangent of its shear angle

$$\tan(\gamma_i) = \frac{u_i - u_{i+1}}{h}, \quad (1 \leq i < M). \quad (31)$$

Results and Discussion

With the use of obtained dependencies, stress-strain state indicators are determined for a rope type RCR-3150 consisting of six cables. The sixth of them is broken. The area length l_0 is assumed equal to 0.1 m. Coefficient of change of shear modulus is 0.5. The results of calculations are given below. Figure 4 shows the dependency of a ratio of internal loads in cables to the average load (coefficients of uneven distribution of forces among the cables) along the x -axis.

Let's pay attention to the fact that $x = 10$ cm corresponds to the boundary of rope parts. Presence of a boundary that divides the rope into parts with different values of shear modulus practically does not affect distribution of forces among the cables. The loads on the broken cable increase as the x -coordinate increases from zero. Cable adjacent to the broken one is loaded more than the other cables. Its maximum internal load – the coefficient of uneven distribution of forces occurs in the cross-section of cable breakage. This value reaches 1.53. The value of coefficients of unevenness decreases with a cable distance from the one adjacent to the broken one and with distance from the cross-section of breakage. We compare the values

of force concentration coefficients for cases of linear and assumed nonlinear dependency of shear modulus on deformations. The analysis of results shows that an increase in the area of action of the reduced shear modulus leads to an increase in the maximum value of coefficient of uneven distribution of forces among cables. Therefore, when rope part length is 100 mm, the excess of the force concentration coefficient reaches 15 %. For a rope part length of 500 mm it reaches 5 %. For the infinite growth of the area of lower rigidity of rubber layers connecting the damaged cable with its adjacent cables, the coefficient of uneven distribution of forces infinitely approaches the corresponding coefficient obtained without considering the nonlinear law of dependency of shear modulus on the mutual shear of cables.

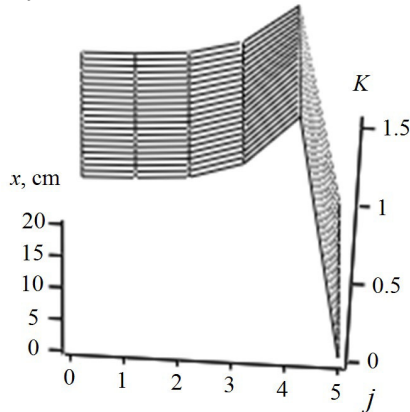


Fig. 4. Dependency of coefficients of uneven distribution of forces among cables with numbers i along x -axis

Butt joints have cross-sections, in which the number of cables changes, just as it changes in a rope with a broken cable. Such a change in the number of cables leads to a mutual displacement of cables in a rope cross-section. The cable with a breakage moves the most relatively to the adjacent ones. This is observed both in butt joints and in a rope with a broken cable. Accordingly, the obtained results can be extended to butt joints. Considering the nonlinearity of rubber shear deformations is expedient because the lengths of butt joint steps are smaller than the sizes of areas of stress disturbance from local change in the butt joint design.

The ratio between displacements of cables numbered i and a displacement of the broken cable in the cross-section of its breakage are shown in the Fig. 5.

The displacements of cables shown in Figure 5 in the cross-section $x=0$ correspond to the assumed form of displacements. As the distance from the cross-section of cable breakage increases, the character of curvature of the rope cross-sections changes - the amount of curvature decreases. The established distribution of displacements made it possible to find distributions of the tangents of shear angles of elastic material between cables. Figure 6 shows the tangents of shear angles of elastic shell between cables with numbers i along the x -axis, relative to its average value.

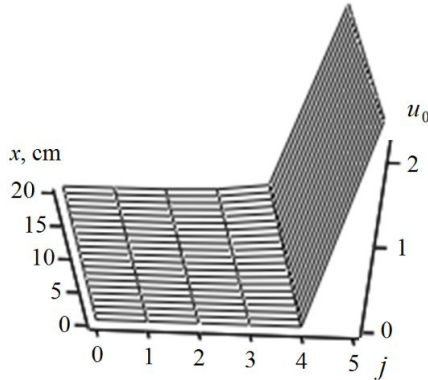


Fig. 5. Dependency of a product of rigidity and displacements of cables with numbers i along x -axis

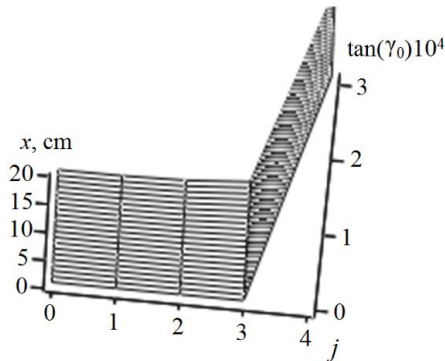


Fig. 6. Dependency of tangents of shear angles of elastic shell between cables with numbers j along x -axis relative to its average value

The shear of cables occurred practically only between the broken cable and the one adjacent to it. At the same time, rigidity of rubber between the specified cables in a rope part ($0 \leq x \leq 10$ mm) is lower than the rigidity of other layers. The maximum mutual shear does not change significantly on the area ($0 \leq x \leq l_0$) (Fig. 7).

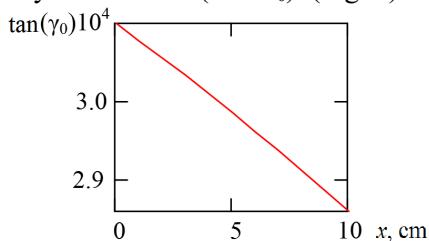


Fig. 7. Dependency of the larger tangents of shear angles of elastic shell between cables along x -axis related to its average value in a rope

Fig. 7 shows a slight deviation of tangents of shear angles of elastic shell from the average value.

In practice, ropes of various designs are used, including with a different number of cables. Fig. 8 shows the dependency of distribution of force distribution coefficients among cables in ropes with different numbers of cables.

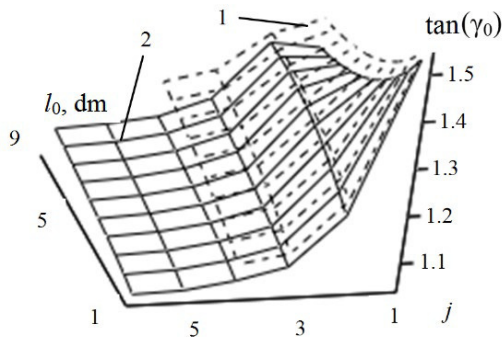


Fig. 8. Coefficients of force distribution among cables in ropes with a different number of cables; 1 - for a rope of five cables, 2 - for a rope of seven cables

The figure shows that an increase in a number of cables in a rope does not significantly affect the maximum values of internal loading forces of cables. The analysis of expressions (27), (28) shows that the increase in the number of cables in a rope over ten practically

does not affect the value of maximum stresses in a case of breakage of the extreme cable. In case of breakage of the middle cable, the maximum force in adjacent cables practically does not depend on their number when there are more than sixteen of them.

Conclusion

By analytically solving a model of a rubber-cable tractive element with a broken structure and nonlinear deformation-dependent rubber shear modulus, the dependencies of changes in a stress state of a rubber-cable tractive element with a broken structure in a form of a cable breakage are established.

In a process of solving the model, an algorithm for determining a stress state of a rubber-cable tractive element with a broken structure is formulated. A mechanism for changing a stress state of a rubber-cable rope is established, considering the nonlinear deformation-dependent shear modulus of rubber.

It is established that an increase in area of action of the reduced shear modulus leads to an increase in the maximum value of a coefficient of uneven distribution of forces between the cables. With infinite growth of area of lower rigidity of rubber layers connecting the broken cable with the adjacent cables, the coefficient of uneven distribution of forces infinitely approaches the corresponding coefficient determined without considering the nonlinear law of the dependency of shear modulus on deformations.

The obtained results can be extended to butt joints. Considering the non-linearity of rubber shear deformations is expedient because lengths of butt joint steps are smaller than sizes of areas of stress disturbance from a local change in butt joint design.

Considering the nonlinear deformation-dependent shear modulus of rubber provides an opportunity to specify the prediction of a rope stress state with a continuity breakage of cables, increase safety and operational reliability of rubber-cable tractive elements.

The results are obtained using well-known methods of theory of composite materials of a rubber-cable rope model and its solution using analytical methods. The model considers the nonlinear law of rubber deformation. This allows considering the obtained results as sufficiently reliable and as such that they clarify the idea of a mechanism of deformation of rubber-cable ropes and belts.

References

1. **Moldabayev, S.K., Adamchuk, A.A., Toktarov, A.A., Aben, Y., Shustov, O.O.** (2020). Approbation of the technology of efficient application of excavator-automobile complexes in the deep open mines. *Naukovyi Visnyk Natsionalnoho Hirnychoho Universytetu*, (4), pp. 30-38. DOI: 10.33271/nvngu/2020-4/030
2. **Pysmennyi, S., Fedko, M., Shvaher, N., Chukharev, S.** (2020). Mining of rich iron ore deposits of complex structure under the conditions of rock pressure development. *E3S Web of Conferences*, 2020, 201, 01022. DOI: 10.1051/e3sconf/202020101022
3. **Tytov, O., Haddad, J., Sukhariev, V.** (2019). Modelling of mined rock thin layer disintegration taking into consideration its properties changing during compaction. *E3S Web of Conferences*, 109, 00105. DOI:10.1051/e3sconf/201910900105
4. **Shustov, O.O., Haddad, J.S., Adamchuk, A.A., Rastsvietaiev, V.O., Cherniaiev, O.V.** (2019). Improving the Construction of Mechanized Complexes for Reloading Points while Developing Deep Open Pits. *Journal of Mining Science*, 2019, 55(6), pp. 946-953. DOI: 10.1134/S1062739119066332
5. **Bondarenko, A.O., Haddad, J.S., Tytov, O.O., Alfaqs, F.** (2021). Complex for processing of rubble wastes of stone dressing. *International Review of Mechanical Engineering*, 15(1), pp. 44-50. DOI: 10.15866/ireme.v15i1.20205
6. **Peremetchyk, A., Kulikovska, O., Shvaher, N., Chukharev, S., Fedorenko, S., Moraru, R., Panayotov, V.** (2022). Predictive geometrization of grade indices of an iron-ore deposit. *Mining of Mineral Deposits*, 16(3), pp. 67-77. DOI: 10.33271/mining16.03.067
7. **Kovalevska, I., Samusia, V., Kolosov, D., Snihur V., Pysmenkova , T.** (2020). Stability of the overworked slightly metamorphosed massif around mine working. *Mining of Mineral Deposits*, 14(2), 43-52. DOI: 10.33271/mining14.02.043
8. **Sotskov, V., Dereviahina, N., & Malanchuk, L.** (2019). Analysis of operation parameters of partial backfilling in the context of selective coal mining. *Mining of Mineral Deposits*, 13(4), 129-138. DOI: [10.33271/mining13.04.129](https://doi.org/10.33271/mining13.04.129)
9. **Shvaher, N., Komisarenko, T., Chukharev, S., Panova, S.** (2019). Annual production enhancement at deep mining. *E3S Web of Conferences*, 123, art. no. 01043. DOI: 10.1051/e3sconf/201912301043
10. **Naumov, V., Zhambabayev, B., Agabekova, D., Zhanbirov, Z., Taran, I.** (2021). Fuzzy-logic approach to estimate the passengers' preference when choosing a bus line within the public transport system. *Communications - Scientific Letters of the University of Žilina*, 23(3), pp. A150-A157. DOI:10.26552/com.C.2021.3.A150-A157
11. **Kravets, V., Samusia, V., Kolosov, D., Bas, K., Onyshchenko, S.** (2020). Discrete mathematical model of travelling wave of conveyor transport. II International Conference Essays of Mining Science and Practic, Vol. 168. DOI: 10.1051/e3sconf/202016800030
12. **Shpachuk, V., Chuprynin, A., Daleka, V., Suprun, T.** (2020). Simulation of impact interaction of rail transport carriage in a Butt Roughness Zone. *Scientific Journal of Silesian University of Technology. Series Transport*, 106, pp. 141-152. DOI:10.20858/sjsutst.2020.106.12

13. **Sladkowski, A.V., Kyrychenko, Y.O., Kogut, P.I., Samusya, V.I., Kolosov, D.L.** (2019). Innovative designs of pumping deep-water hydrolifts based on progressive multiphase non-equilibrium models. *Naukovyi Visnyk Natsionalnoho Hirnychoho Universytetu*, (2), pp. 51-57. DOI: 10.29202/nvngu/2019-2/6
14. **Bondarenko, A.O., Maliarenko, P.O., Zapara, Ye., Bliskun, S.P.** (2020). Testing of the complex for gravitational washing of sand. *Naukovyi Visnyk Natsionalnoho Hirnychoho Universytetu*, (5), 26-32. DOI: 10.33271/nvngu/2020-5/026
15. **Shpachuk, V.P., Zasiadko, M.A., Dudko, V.V.** (2018). Investigation of stress-strain state of packet node connection in spatial vibration shakers. *Naukovyi Visnyk Natsionalnoho Hirnychoho Universytetu*, (3), 74-79. DOI: 10.29202/nvngu/2018-3/12
16. **Bazhenov, V.A., Gulyar, A.I., Piskunov, S.O., Shkryl, A.A.** (2006). Life assessment for a gas turbine blade under creep conditions based on continuum fracture mechanics. *Strength of Materials*, 38(4), pp. 392-397.
17. **Bazhenov, V.A., Gulyar, A.I., Piskunov, S.O., Shkryl, A.A.** (2008). Gas turbine blade service life assessment with account of fracture stage. *Strength of Materials*, 2008, 40(5), pp. 518-524.
18. **Vynohradov, B.V., Samusya, V.I., Kolosov, D.L.** (2019). Limitation of oscillations of vibrating machines during start-up and shutdown. *Naukovyi Visnyk Natsionalnoho Hirnychoho Universytetu*, (1), pp. 69-75. DOI: 10.29202/nvngu/2019-1/6
19. **Chigirinsky, V., Naumenko, O.** (2020). Invariant Differential Generalizations in Problems of the Elasticity Theory As Applied to Polar Coordinates. *Eastern-European Journal of Enterprise Technologies*, 5(7 (107)), 56-73. DOI: 10.15587/1729-4061.2020.213476
20. **Marasová, D., Ambriško, L., Andrejiová, M., Grinčová, A.** (2017). Examination of the process of damaging the top covering layer of a conveyor belt applying the FEM. *Journal of the International Measurement Confederation*, (112), 47-52. DOI:10.1016/j.measurement.2017.08.016
21. **Belmas, I., Kogut, P., Kolosov, D., Samusia, V., Onyshchenko, S.** (2019). Rigidity of elastic shell of rubber-cable belt during displacement of cables relatively to drum. *International Conference Essays of Mining Science and Practice*, Vol. 109, 00005. DOI: 10.1051/e3sconf/201910900005
22. **Blazej, R., Jurdziak, L., Kirjanow-Blazej, A.** et al. (2021). Identification of damage development in the core of steel cord belts with the diagnostic system. *Sci Rep* 11, 12349. DOI: 10.1038/s41598-021-91538-z
23. **Webb, C., Sikorska, J., Khan, R., & Hodkiewicz, M.** (2020). Developing and evaluating predictive conveyor belt wear models. *Data-Centric Engineering*, 1, E3. DOI: 10.1017/dce.2020.1
24. **Pang, Y., Lodewijks, G.** (2006). A Novel Embedded Conductive Detection System for Intelligent Conveyor Belt Monitoring. 2006 IEEE International Conference on Service Operations and Logistics, and Informatics, SOLI 2006. 803-808. DOI: 10.1109/SOLI.2006.328958

25. **Volohovskiy, V.Yu., Radin, V.P., & Rudyak, M.B.** (2010). Concentration of loads in cables and a bearing ability of rubber-cable conveyor belts with breakages. *MPEI Vestnik*, (5), 5-12.
26. **Bel'mas, I.V.** (1993). Stress state of rubber-rope tapes during their random damages. *Problemy Prochnosti i Nadezhnos'ti Mashin*, 1993, (6), pp. 45-48.
27. **Ropay V.A.** (2016) *Shakhtnyye uravnoveshivayushchiye kanaty: monograph [Mining balancing ropes]*. Dnipropetrovsk : National Mining University. 263 p.
28. **Levchenya, Zh.B.** (2004). Increase of reliability of butt-joint connections of conveyor belts at mining enterprises: PhD dissertation: 05.05.06.
29. **Kolosov, L.V., Bel'mas, I.V.** (1981). Use of electrical models for investigating composites. *Mechanics of Composite Materials*, 1981, 17(1), pp. 115-119.
30. **Daria Zade S.** (2013). Numerical method of determining effective characteristics of unidirectional reinforced composites. *Bulletin NTU "KhPI"*, (58), 71-77.
31. **W. Song, W. Shang and X. Li,** (2009). Finite element analysis of steel cord conveyor belt splice. *International Technology and Innovation Conference 2009 (ITIC 2009)*, Xi'an, China, pp. 1-6. DOI: 10.1049/cp.2009.1415
32. **Xianguo Li, Xinyu Long, Zhenqian Shen, Changyun Miao** (2019). Analysis of Strength Factors of Steel Cord Conveyor Belt Splices Based on the FEM. *Advances in Materials Science and Engineering*, Volume 2019, ID 6926413. DOI: 10.1155/2019/6926413
33. **Fedorko, G., Molnar, V., Michalik, P., Dovica, M., Kelemenová, T., Toth, T.** (2018). Failure analysis of conveyor belt samples under tensile load. *Journal of Industrial Textiles*. 48. 152808371876377. DOI: 10.1177/1528083718763776
34. **Andrejiova, M., Grincova, A., Marasova, D.** (2019). Failure analysis of the rubber-textile conveyor belts using classification models. *Engineering Failure Analysis*. 101. 407-417. DOI: 10.1016/j.engfailanal.2019.04.001
35. **Belmas I.V., Kolosov D.L., Kolosov A.L., Onyshchenko S.V.** (2018). Stress-strain state of rubber-cable tractive element of tubular shape. *Naukovyi Visnyk Natsionalnoho Hirnychoho Universytetu*, (2), pp. 60-69. DOI: 10.29202/nvngu/2018-2/5
36. **Kirjanów-Błażej, A., Błażej, R. Jurdziak, L., Kozłowski, T.** (2017). Core damage increase assessment in the conveyor belt with steel cords. *Diagnostyka*. 18. 93-98.
37. **Romek D., Ulbrich D., Selech J., Kowalczyk J., Wład R.** (2021). Assessment of Padding Elements Wear of Belt Conveyors Working in Combination of Rubber-Quartz-Metal Condition. *Materials (Basel)*. Aug 2;14(15):4323. DOI: 10.3390/ma14154323
38. **Yao Y., Zhang B.** (2020). Influence of the elastic modulus of a conveyor belt on the power allocation of multi-drive conveyors. *PLoS One*. Jul 7; 15(7):e0235768. DOI: 10.1371/journal.pone.0235768
39. **Zabolotny, K.S., Panchenko, E.V., Zhupiev, A.L.** (2011). *Teoriya mnog-osloynnoy namotki rezinotrosovogo kanata [Theory of multilayer rubber-cable rope winding]*. Dnipropetrovsk: NGU.
40. **Haddad, J.S., Denyshchenko, O., Kolosov, D., Bartashevskiy, S., Rastsvietaiev, V., & Cherniaiev, O.** (2021). Reducing Wear of the Mine Ropeways Components Basing Upon the Studies of Their Contact Interaction. *Archives of Mining Sciences*, 66(4), 579-594. DOI: 10.24425/ams.2021.139598